Stony Brook University

Characterizing the lipoproteins LprG and LprA towards a better understanding of lipid transport mechanisms in *Mycobacterium tuberculosis*

A Thesis Presented

by

Lu Bai

to

The Graduate School

in Partial Fulfillment of the

Requirements

for the Degree of

Master of Science

in

Chemistry

Stony Brook University

August 2013

Stony Brook University

The Graduate School

Lu Bai

We, the thesis committee for the above candidate for the

Master of Science degree, hereby recommend

acceptance of this thesis.

Jessica Seeliger, Ph. D. – Thesis Advisor
Assistant Professor, Department of Pharmacological Sciences

Peter Tonge, Ph. D. – Chairperson of the Thesis Committee
Professor, Department of Chemistry

Erwin London, Ph. D. – Third Member of the Thesis Committee

This thesis is accepted by the Graduate School

Charles Taber
Interim Dean of the Graduate School

Abstract of the Thesis

Characterizing the lipoproteins LprG and LprA towards a better understanding of lipid transport mechanisms in *Mycobacterium tuberculosis*

by

Lu Bai

Master of Science

in

Chemistry

Stony Brook University

2013

Two lipoproteins, MtbLprG and MtbLprA, have been characterized as TLR2 agonists. Knockout of the *lprG* operon (*lprG-rv1410c*) results in decreased virulence of *M. tb*. While their importance for host-pathogen interactions has been the subject of numerous studies, the physiological functions of LprG and LprA are not known. We present here data towards elucidating the physiological functions of LprG and LprA, both in *M. tb* and *M. smegmatis*, including localization, binding affinity to respective ligands, as well as the phenotype of knockout strains, which will contribute a model for lipid transport through the cell wall.

Table of Contents

List of Figures

List of Tables

List of Abbreviations

TB: Tuberculosis

MDR-TB: Multidrug-resistant TB

TLR2: Toll-like Receptor 2

PRRs: Pattern Recognition Receptors

Lgt: Pre-prolipoprotein Diglyceryl Transferase

Lsp: Prolipoprotein Signal Peptidase

Lnt: Apolipoprotein N-acyl Transferase

PI: Phosphatidyl Inositol

PIMs: Phosphatidyl-inositol Mannosides

LM: Lipomannan

LAM: Lipoarabinomannan

PDIM: Phthiocerol Dimycocerosates

K_d: Dissociation Constant

NA: Non-acylated

LB: Luria-Bertani broth

FPLC: Fast Protein Liquid Chromatography

CV: Column Volume

NBD-SA: 12-N-methyl-(7-nitrobenz-2-oxa-1,3-diazo) Aminostearic Acid

PBS: Phosphate-buffered Saline

CW: Cell Wall-enriched Fraction

CM: Inner Membrane-enriched Fraction

CYT: Cytosol-enriched Fraction

Anti-WCL: Anti-Whole Cell Lysate

MVs: Membrane Vesicles

ITC: Isothermal Titration Calorimetry

SPR: Surface Plasmon Resonance

BLI: Bio-layer Interferometry

Chapter 1. Introduction

1.1 Mycobacterium tuberculosis

Tuberculosis (TB) is an infectious disease caused by the bacterium *Mycobacterium tuberculosis* (*M. tb*) and remains a major global health problem. It infects one-third of the global population and ranks as the second leading cause of death from an infectious disease worldwide, after the human immunodeficiency virus (HIV). The probability of developing TB is much higher among people infected with HIV. Although the world is on track to achieve the Millennium Development Goal (MDG) target to halve 1990 levels of mortality by 2015 and new cases have been falling for several years, the global burden of TB remains enormous. The latest estimates from the 2012 Global Tuberculosis Report are that there were 8.7 million new cases in 2011 (13% co-infected with HIV) and 1.4 million TB-related deaths[1].

Treatment for new cases of drug-susceptible TB consists of a 6-month regimen of four first-line drugs: isoniazid, rifampicin, ethambutol and pyrazinamide. Treatment for multidrug-resistant TB (MDR-TB), defined as resistance to isoniazid and rifampicin (the two most powerful anti-TB drugs) is longer, and requires more expensive and toxic drugs. For most patients with MDR-TB, the current regimens recommended by the WHO last 20 months. The public health crisis posed by TB, as well as the current long and high-cost treatment, especially for multidrug-resistant TB, requires new therapeutic strategies and therefore a better understanding of both the pathogen and the host response.

1.2 Toll-like Receptor 2 (TLR2) is an important contributor to innate immune recognition of *M. tb*

Since *M. tb* survive within cells of the innate immune system, this interaction is likely crucial to the establishment and maintenance of the balance between host and pathogen. The innate immune response against *M. tb* begins with the inhalation of bacilli into the lungs where they are recognized by the pattern recognition receptors (PRRs) of alveolar macrophages, dendritic cells, and monocytes. Recognition of *M. tb* by PRRs is mediated primarily by Toll-like receptors (TLRs), especially TLR2, TLR4, and TLR9. It has been reported that the response to *M. tb* by macrophages is mediated primarily by TLR2[2].

Interactions between TLR2 and *M. tb* ligands can activate functions that promote the killing of the bacteria. On the other hand, TLR2 agonists produced by *M. tb* can also decrease processing and presentation of antigen by down-regulating the levels of MHCII molecules on macrophages and dendritic cells through long-term TLR2 signaling[3].

At least two classes of molecules produced by *Mycobacteria* can be sensed by TLR2: lipoproteins and glycolipids. The two lipoproteins discussed in this thesis, MtbLprG and MtbLprA, have been characterized as TLR2 agonists[3,4].

MtbLprG and MtbLprA are homologous lipoproteins in *M. tb*. These N-terminally triacylated lipoproteins contain a N-terminal secretion signal peptide and a lipobox motif

for lipid modification on a conserved cysteine. The secretion signal sequence directs preprolipoprotein transport through the plasma membrane where a diacyglyceride unit is added to the cysteine via a thioether bond by the enzyme pre-prolipoprotein diglyceryl transferase (Lgt). The signal sequence is then cleaved by prolipoprotein signal peptidase (Lsp) and a third acyl chain is attached to the amino terminus of N-terminal cysteine by apolipoprotein n-acyl transferase (Lnt)[5].

1.3 LprG and LprA can associate with PI-based glycolipids, which are also TLR2 agonists

Using immunoblotting and mass spectrometry analysis, MtbLprG isolated from *M. smegmatis* was detected as associating with lipoarabinomannan (LAM), lipomannan (LM), phosphatidyl-inositol mannosides (PIMs), as well as phosphatidyl inositol (PI)[6]. PI was also detected in association with LprA by LC-MS[6]. The TLR2 agonist activity of LprG is dependent on their association with phosphatidyl inositol-based (PI-based) glycolipids.

PI-based glycolipids from mycobacteria include LAM, LM, and PIMs. They are major lipoglycans in the *mycobacteria* cell envelope and are also characterized as TLR2 agonists[7,8]. These glycolipids are believed to be synthesized in the cytosol or plasma membrane. After synthesis, the lipoglycans are transferred to the outer membrane, where they noncovalently intercalate into the outer leaflet of the outer membrane and are exposed at the cell surface[9,10].

The co-crystal structure of MtbLprG with Ac_1PIM_2 (Fig. 1-1) shows that it has a β-sheet composed of ten antiparallel strands on one side and 6 α-helices on the opposite side. The cavity and the entrance are lined primarily with the side chains of hydrophobic residues. Introduction of a bulky tryptophan in the putative binding pocket blocks association of glycolipids. The hydrophobic pocket structure of LprG supports its ability to bind lipids.

Although LprA and LprG are homologous and have 34% sequence identity, when the predicted structure of LprA was generated using MtbLprG as template, residues in LprA were found to define a narrower pocket opening and overlap with the structure of PIM^5, which may explain why only the smaller lipid PI was detected in association with LprA. This suggests that the binding of lipoproteins to PIM family ligands has high specificity.

LppX, a lipoprotein homologous with LprG and LprA, has been implicated in the transport of phthiocerol dimycocerosates (PDIM) to the surface of *M. tb*[11]. Although no in vitro binding data is available, lipid analysis revealed that the Δ*lppX* mutant fails to release PDIM into the culture medium. The function of LppX in PDIM trafficking is likewise supported by its hydrophobic cavity structure. The sequence homology with LppX provides additional evidence for LprG and LprA in their hypothesized participation in lipid transport and cell wall assembly.

LprG, LprA and LppX belong to a family of predicted lipoproteins with predicted homologous structures. This family has homologues in species of the *M. tb* complex. In contrast, the non-pathogenic species *M. smegmatis* has only one homologue, LprG.

1.4 Knockout of *lprG* operon (*lprG-rv1410c*) results in decreased virulence of *M. tb*

In both *M. smegmatis* and *M. tb*, the two genes *lprG* and *rv1410c* form an operon, and they encode two proteins, LprG and P55, that are a predicted lipoprotein and a predicted transporter, respectively[12]. In *M. smegmatis*, the *lprG-rv1410c* operon is required for resistance to ethidium bromide[13], which implies that membrane integrity may be compromised in the knockout. The operon is also important for virulence since knocking out this operon results in decreased virulence of *M. tb*[14]. Additional studies have demonstrated that *M. smegmatis* mc^2 155 lacking this operon is defective for sliding motility, indicating that the proteins may function together in construction of the mycobacterial envelope[13].

While their importance for host-pathogen interactions has been the subject of numerous studies, the physiological functions of LprG and LprA are not known. Based on the results of immunology studies, their ability to bind to lipids, as well as the MtbLprG crystal structure, we hypothesize that LprG and LprA function as carriers of phosphatidyl inositol-derived glycolipids (PIMs, AcPIMs, LM and LAM) during their trafficking and delivery to the outer membrane. Here we present data towards elucidating the physiological functions of LprG and LprA, both in *M. tb* and *M. smegmatis*, including localization, ligands binding affinity, as well as the phenotype of knockout strains. These

data would contribute to understanding the mechanism of lipid transport through the cell wall.

The subcellular localization of LprG and LprA was determined using fractionation methods and immunoblotting. Full-length proteins were all detected in the cytosolic membrane- and cell wall-enriched fractions, which is consistent with their prediction as lipoproteins and our hypothesis.

To measure binding affinities of LprG and LprA for their respective ligands, we performed preliminary studies on a fluorescence-based assay to measure competitive binding of LprG with LM and LAM. Though the determination of the dissociation constant (K_d) of LprG and LprA to respective ligands is still in progress, differences between the lipid-binding affinities of these lipoproteins were detected by binding with a fluorescent reporter lipid.

Towards the verification of LprG binding to LAM/LM in mycobacteria, we elucidated the phenotype of *M.smegmatis lprG-rv1410c* knockout strains with respect to LAM localization. Our preliminary results suggest that LprG and Rv1410 may be redundant or are not involved in LAM transport to the outer membrane.

Chapter 2. Materials and Methods

2.1 Cloning

MtbLprG was amplified from *M. tb* H37Rv genomic DNA by touchdown PCR using the following primers (sequences written 5′ to 3′; underlined portions are NdeI and HindIII restriction enzyme recognition sites, and the TEV protease recognition site): the 5′ primer AAGAAGGAGATATACATATGCGGACCCCCAGACG and the 3′ primer GTGCGGCCGCAAGCTTGGATTGGAAGTACAGGTTTTCGCTCACCGGGGGCTT C. A non-acylated (NA) version of LprG that excludes the signal sequence and changes the acylated cysteine to a methionine was cloned using the following primers: the 5′ primer AAGAAGGAGATATACATATGTCGTCGGGCTCGAAGCC and the 3′ primer GTGCGGCCGCAAGCTTGGATTGGAAGTACAGGTTTTCGCTCACCGGGGGCTT C. Site-directed mutagenesis of full-length MtbLprG and NA-MtbLprG was performed with the 5′ primer GCCGCGACGGGAAACTGGAAGCTCACGCTGGGT and the 3′ primer ACCCAGCGTGAGCTTCCAGTTTCCCGTCGCGGC. The underlined portion is the mutation site. The amino acid was mutated from valine to tryptophan.

For expression in *E. coli*, the target gene was inserted into the pET24b vector using ligation-independent cloning (Clontech InFusion). The target gene was placed behind the IPTG-inducible T7-lac promoter and in frame with a TEV protease recognition site and a C-terminal His_6-tag. The plasmid was then transformed to *E. coli* Stellar competent cells for DNA amplification.

For expression in *M. smegmatis*, MtbLprG subcloned using the following primers (underlined portions are MscI and EcoRI restriction enzyme recognition sites): the 5′

primer AAGGAGGCAACAAGATGGCCAGCCGGACCCCCAGACGCC and the 3′ primer GACATCGATAAGCTTGAATTCCTTTGTTAGCAGCCGGATCTCAGTG. Using the same method mentioned above, the gene sequences were inserted into the pRibo EcoHind[15] in-frame with a TEV protease recognition site and a C-terminal His_6-tag.

For constitutive expression, MtbLprG was cloned into pMV261 for constitutive expression[16]. Target genes were amplified from the pET24b constructs described above using the following primers (underlined portions are MscI and EcoRI restriction enzyme recognition sites): the 5′ primer GGAATCACTTCGCAATGGCCAGCCGGACCCCCAGACGCC and the 3′ primer ACATCGATAAGCTTCGAATTCCTTTGTTAGCAGCCGGATCTCAGTG. Using the same method mentioned above, the gene sequences were inserted into pMV261 verctor behind the constitutively active *hsp60* promoter and in-frame with a TEV protease recognition site and a C-terminal His_6-tag.

The non-acylated (NA) version of LprG, as well as the mutants, was also subcloned into the pRibo EcoHind and pMV261 vectors. (Refer to Table 1 in appendix for primer sequences and methods.)

Full-length and non-acylated versions of MtbLprA were amplified from *M.tb* H37Rv genomic DNA and cloned into pET24b and pRibo EcoHind vectors as above. MsmegLprG and the non-acylated version were amplified from *M. smegmatis* genomic

DNA and constructed into pET24b, pRibo EcoHind, and pMV261 vectors as above. (Refer to appendix for primer sequences and methods.)

2.2 Overexpression of His_6-tagged recombinant proteins

For expression in *E. coli*, BL21(DE3) competent cells were transformed with the pET24b constructs and cultured in Luria-Bertani broth (LB); 50 μg/mL kanamycin was used for selection. When the OD_{600} was approximately 1, 0.1 mM IPTG was added to induce protein expression for 4 h at 37 °C or 16 h at 18 °C. Bacteria were isolated by centrifugation at 5000 xg for 20 min at 4 °C. The pellet was stored at -20 °C or lysed immediately. (Refer to Table 2 in appendix for expression conditions used for specific proteins.)

For expression in *M. smegmatis*, strain mc^2155 was transformed by electroporation with a Gene Pulser II apparatus (Bio-Rad) set to 2.5 kV, 25 μF and 800 Ω. *M. smegmatis* was cultured in Middlebrook 7H9 (supplemented with 10% ADC, 0.5% glycerol and 0.05% Tween 80) or Sauton medium; 25 μg/mL kanamycin was used for selection. Protein expression was induced for 6 h at 37 °C by addition of 2 mM theophylline.

2.3 Purification of His_6-tagged proteins

All steps were performed at 4 °C unless otherwise noted. Cell pellets were resuspended in lysis buffer (20 mM Tris, 200 mM NaCl, 1 mM EDTA, 1 mM DTT, pH 7.4) and sonicated 5s on/off for 10 min total processing time. Insoluble material was removed by centrifugation at 12,000 xg for 1 h at 4 °C. After filtering through a 0.45 µm filter, the whole cell lysate was subjected to fast protein liquid chromatography (FPLC).

Nickel affinity chromatography (HisTrap FF 5mL, GE Healthcare) was used for initial purification. After injection, protein samples were washed with 5 column volume (CV) binding buffer (Buffer A, 50 mM Tris, 1 mM DTT, 10% glycerol, pH 7.4), and bound proteins were eluted with a 0-50% gradient of elution buffer (Buffer A with 1M imidazole) over 20 CV. All target proteins eluted at an imidazole concentration of approximately 100 mM and were analyzed for purity by SDS-PAGE. If contaminating proteins co-eluted, a second purification step by anion exchange chromatography (HiTrap Q HP 5 mL, GE Healthcare) was performed. The protein was eluted with a gradient of 0-100% high salt buffer (Buffer A with 1M NaCl) over 20 CV. The pH of the buffer was adjusted to at least 1 unit higher than the theoretical isoelectric point (pI) of the target protein (Refer to table 2 in appendix for protein theoretical pI). All of the proteins were purified in a final step by size exclusion (HiPrep 16/60 120 mL, GE Healthcare). The mobile phase was buffer A without glycerol. Purified proteins were verified by tryptic digest and mass spectrometry (MS), flash frozen in liquid nitrogen and stored at -80 °C in Buffer A. Using the theoretical extinction coefficient, proteins' concentrations were estimated by A_{280}. (Refer to table 2 in appendix for theoretical extinction coefficient of each protein.)

All of the non-acylated proteins (NA-MtbLprG, V91W NA-MtbLprG, NA-MtbLprA, and NA-MsmegLprG) were stably expressed in *E. coli* and purified and verified by MS as described above. For full-length proteins, only MtbLprA was verified by MS. (Refer to table 2 in appendix for purification conditions used for specific proteins.)

2.4 Fluorescence Assay

2.4.1 Direct binding to a fluorescent reporter lipid

The assay was set up in 96-well black plate with black bottom. To measure direct binding between protein and fluorescent probe, the concentration of the fluorescent fatty acid, NBD-SA (12-N-methyl-(7-nitrobenz-2-oxa-1,3-diazo) aminostearic acid) (Fig. 2-1), was held constant at 200 nM and the concentration of protein was varied between 0 and 80μM. The total volume in each well was 200 μL and all measurements were taken using binding buffer (50 mM Tris, 1 mM DTT, 100 mM NaCl, pH 8.0). Buffer alone and buffer containing 200 nM probe served as negative controls. The plates were read using a Spectramax M2a plate reader (Molecular Devices). The excitation wavelength was 466nm and the emission was measured from 500 nm to 600 nm in 10 nm increments with a cut-off at 515 nm. Assays were performed in triplicate and binding curves were fit the equation:

$$y=m_3+m_2\times m_0/(m_1+m_0)$$

using Kaleidagraph (Synergy Software) where y is the fractional occupancy, m_0 is the protein concentration, $m_1$is the dissociation constant (K_d) and m_2 is the scale factor.

2.4.2 Competitive binding assay with putative ligands

To detect binding between NA-MtbLprG and LM or ManLAM, 200 nM NBD-SA and 10 μM wild-type or V91W NA-MtbLprG were incubated. The concentration of LM and MamLAM was varied between 0 and 10 μM. Buffer only, buffer containing 200 nM probe, and buffer containing 200 nM probe and 10 μM ligand were prepared as negative controls. The parameters used in fluorescence detection were the same as described above.

2.5 Subcellular Fractionation

M. smegmatis expressing full-length and non-acylated MtbLprG, MtbLprA and MsmegLprG were grown to OD 0.8 as described (see above, Overexpression). Cells from a 100-mL culture were harvested and washed three times with phosphate-buffered saline (PBS), resuspended in 3 mL PBS, and sonicated (5 s on/off, 8 min total processing time) in an ice bath. The lysates were spun at 1000 xg for 10 min to remove unbroken cells and fractionated by differential centrifugation fractionation methods.

The total lysate was fractionated as previously described[17] and all steps were performed at 4 °C. Briefly, the lysates were subjected to ultracentrifugation at 27,000 xg for 4 h to pellet the cell wall-enriched (CW) fraction. As the resulting pellet may still

contain unbroken cells, the pellet was resuspended in 3 mL PBS and lysed as above a second time. The resulting supernatant was centrifuged at 27,000 xg to yield a second CW pellet. The supernatants were pooled and centrifuged at 100,000 xg for 1 h. The resulting pellet is the inner membrane-enriched fraction (CM) while the supernatant is enriched for cytosolic proteins (CYT). The protein concentrations of each fraction were determined by the bicinchoninic acid assay (BCA Assay, Pierce).

M. smegmatis wild type mc^2155, Δ*lprG-rv1410c*, and Δ*lprG-rv1410c::MtblprG-rv1410c* strains[13] (gift of Eric J. Rubin, Harvard School of Public Health) were grown to OD_{600} 1-1.5, lysed, and fractionated by differential centrifugation as described above to obtain cytosol-, inner membrane- and cell wall-enriched fractions.

2.6 Immunoblotting

Proteins were separated by SDS-PAGE gel and transferred to nitrocellulose membranes (Mini-Protean system, Bio-Rad) at 100V for 2 h or 26 V overnight at 4 °C. Membranes were blocked with 5% non-fat milk in water at room temperature for 1h if visualized by chemiluminescence or blocked with Odyssey blocking buffer (LI-COR Biosciences) overnight at 4 °C if visualized by fluorescence (Odyssey scanner, LI-COR Biosciences).

For His-tag detection, 1 μg of protein from each fraction was separated by SDS-PAGE. Anti-Histag antibody fused with HRP (ab1187, abcam) was diluted 1:10,000 in

5% non-fat milk and incubated with the membrane for 1 h at room temperature. The membrane was washed with TBST (100 mM Tris, 154 mM NaCl, 0.05% Tween 20, pH 8.0) 4 times for 10 min each. The membrane was incubated for 2 min with substrate (Immobilon, Millipore) and exposed to film for 5 s, 10 s, 30 s, or 30 min.

For MspA detection, samples were extracted with 0.6% octylthioglucoside (OTG, AC230340010, Acros Organics) in PBS at 98 °C for 30 min. Samples were then cooled on ice for 10 min and centrifuged at 4000 xg for 10 min. A total of 200 ng protein for each subcellular fraction was separated by SDS-PAGE. Blots were probed with anti-MspA antibody (1:500 in Odyssey blocking buffer; gift of M. Niederweis, University of Alabama, Birmingham[18]). The secondary antibody was goat anti-rabbit IR700 (1:10,000 in Odyssey blocking buffer, LI-COR Biosciences).

For KatG detection, 5 µg of protein from each fraction was separated by SDS-PAGE. Membranes were probed with anti-KatG CS57 (1:500 in Odyssey blocking buffer; NR-13793, BEI Resources). Goat anti-mouse IR800 (1:15,000 in Odyssey blocking buffer, LI-COR Biosciences) was used as secondary antibody if the membrane was visualized by fluorescence. Anti-mouse HRP (1:2,000 in 5% non-fat milk, LI-COR Biosciences) was used if visualized by chemiluminescence.

For *M. smegmatis* LAM detection, 5 µg of protein from each fraction was separated by SDS-PAGE. After transfer, membranes were probed with anti-smegLAM (1:20 in Odyssey blocking buffer/PBS; NR-13798, BEI Resources) and anti-Whole Cell

Lysate (anti-WCL) (1:2,000 in Odyssey blocking buffer/PBS; NR-13819 BEI Resources). The secondary antibody was goat anti-mouse IR800 (1:15,000 in Odyssey blocking buffer, LI-COR Biosciences) for anti-smegLAM or goat anti-rabbit IR700 (1:10,000 in Odyssey blocking buffer, LI-COR Biosciences) for anti-WCL. The membranes were visualized by fluorescence.

Chapter 3. Results and Discussion

3.1 Protein Localization

M. smegmatis is a fast growing non-pathogenic mycobacterial species with similar protein secretion systems as *M. tb*. Therefore, *M. smegmatis* was chosen as the expression host for our protein localization studies in mycobacteria[19].

To test our hypothesis that LprG and LprA are associated with the cell envelope, we determined their subcellular locations by fractionating *M. smegmatis* cells expressing full-length or non-acylated versions of MtbLprG, MtbLprA, and MsmegLprG with a C-terminal His_6-tag. Differential centrifugation fractionation method was used for characterizing the subcellular locations of each protein. To verify the fractionation results, KatG and MspA were used as cytosolic and outer membrane markers, respectively. Using a differential centrifugation fractionation method[17], KatG was detected only in the cytosol fraction and MspA was enriched in the outer membrane fraction (Fig. 3-1), as expected.

Consistent with their prediction as lipoproteins, the full-length proteins were all detected in the cytosolic membrane- and cell wall-enriched fractions using the differential centrifugation fractionation method (Fig. 3-1). Although previous studies showed that MtbLprG and LprA could be secreted into the environment through membrane vesicles (MVs)[20], these two lipoproteins were not detected in the culture filtrate. As *M. smegmatis* is a non-pathogenic strain, and no lipoproteins have been detected in *M. smegmatis* membrane vesicles in constract to *M. tb*, *M. smegmatis* may not be capable of secreting these proteins in the same manner as *M. tb*.

Non-acylated proteins were only detected in cytosol-enriched fraction (Fig. 3-1). This result is consistent with mechanism of lipoprotein export: the sequence upstream of the conserved cysteine is a putative secretion signal, without which the protein should remain in the cytosol.

In summary, MtbLprG, MsmegLprG and MtbLprA are cell wall-associated proteins. The location of these lipoproteins is consistent with the cell envelope model and our hypothesis that they may function as carriers of phosphatidyl inositol-derived glycolipids during their trafficking and delivery to the outer membrane.

3.2 Binding

Consistent with the predicted low solubility of these lipoproteins due to their N-terminal signal sequence, the full-length proteins were more difficult to express and purify from *E. coli* than their non-acylated counterparts. Thus, non-acylated proteins were

used for all binding assays unless otherwise noted. Modified conditions may need to be developed for the expression and purification of acylated proteins in the future.

To measure binding affinities of LprG and LprA for their respective ligands, the fluorescent fatty acid (Fig. 2-1) was used as a fluorescent probe in binding assays with non-acylated MtbLprG, V91W MtbLprG, MsmegLprG and MtbLprA. Based on the binding curve and K_d of the probe with individual proteins and modeling of the competitive binding curve[21], a fixed concentration of NBD-SA (200 nM) and protein (10 μM) were pre-incubated for the competitive binding assay. In this assay a second (non-fluorescent) ligand is titrated against the pre-formed complex and concentration-dependent displacement of NBD-SA is detected as a decrease in detected signal. The K_d for the competing ligand is then calculated based on a model of competitive binding[21] and the K_d for direct binding to NBD-SA. Using this condition for competitive binding assay, it is expected to get a sufficient fluorescence signal and detect a significant signal decrease if the K_d of protein to non-fluorescent ligand is approximately 1 μM.

For direct binding of proteins to NBD-SA, the dissociation constants are listed in Table 3-1. Though previous studies indicate that the V91W mutation in MtbLprG blocks the binding of triacylated lipid ligands of the PIM family[6], NA-MtbLprG (K_d=5±1.1 μM) and V91W mutated NA-MtbLprG (K_d=6±1.6 μM) bind to NBD-SA with comparable dissociation constants (Fig. 3-2). Compared to the putative native ligands, which are modified with two to three fatty acid acylchains, NBD-SA has one fatty acid chain with 18 carbons. Therefore, the single V91W mutation may be insufficient to block the

binding of a single-chain fatty acid to the protein. As NBD-SA can bind to the V91W mutant, it could be used in the competitive binding assay to compare the binding affinity of native and mutated proteins with proposed PIM-family ligands.

The fluorescent probe binds more tightly to NA-MtbLprG (K_d=5±1.1 μM) than to MsmegLprG (K_d=26±10.8 μM) (Fig. 3-2). This result implies that the binding pockets of MtbLprG and MsmegLprG may differ significantly, although these two proteins are highly homologous (54% i.d.). Figure 3-3 shows the surface inside the predicted binding pocket of MtbLprG (PDB ID: 3MHA) and MsmegLprG (structure prediction generated using the Phyre2 server using MtbLprG as a template). At the putative entrance to the binding pocket, position 96 is a phenylalanine in MsmegLprG, compared to a glycine in MtbLprG. This bulky phenylalanine may affect the binding of multiply acylated lipids to the protein. For MsmegLprG, position 71 is proline, whereas it is leucine in MtbLprG. This hydrophilic residue in the pocket entrance may also influence the affinity of lipid binding to protein. This structural analysis of MtbLprG and MsmegLprG shows differences in hydrophobicity, as well as the shape and size of binding pockets, which may contribute to their different binding affinity to NBD-SA. Future analysis will include comparisons of cavity size and the identification of residues that differ between the two proteins and, along those mentioned above, may determine the differences in binding affinity, as well as ligand specificity.

The sequence homology and operon structure of MtbLprG and MsmegLprG imply identical activity and similar binding affinity, but this is contradicted by the

binding data with NBD-SA. Therefore, future directions will include elucidation of ligand-binding specificity by expressing both MtbLprG and MsmegLprG in *M. smegmatis* and *M. marinum*, a pathogenic mycobacterial species that is closely related to M. tb. With immunoblotting and MS analysis, ligands other than PIM's family might be detected, which would assist further comparison of the binding specificities of these two proteins.

Competitive bindings of NA-MtbLprG with MtbLM, MtbLAM, as well as the bindings of V91W NA-MtbLprG with MtbLM and MtbLAM, were measured (Fig. 3-4). For the competitive binding assay, no significant decrease in signal was detected for any of the ligand-protein combinations. The fluorescence signal increased with increasing competitive ligand concentration. Also, high background signal from NBD-SA was observed in the presence of competitive ligand alone. The fluorescence signal of 200 nM NBD-SA with 10 μM LM was 87 RFU, and with 10 μM LAM, the signal was 171 RFU. The background is sufficiently high to interfere with any observation of NBD-SA displacement in the LprG binding pocket. As LM and LAM have fatty acid chains, they may form micelles or vesicles in the buffer. The background fluorescence signal is most likely caused by the association of NBD-SA with micelles or vesicles formed by LM and LAM.

Though the fluorescence assay is known to be an efficient method with high sensitivity and relatively low cost, it may not be a good choice to measure the binding affinities in our case due to the high background signal. Also, compared with the fatty-

acid proteins examined in published fluorescence assays with NBD-SA, the binding pocket is much larger in MtbLprG, so the fluorescent probe and the ligands may bind to the protein at the same time.

Based on these results, other methods should be considered or developed for the binding affinity assay. These alternatives include isothermal titration calorimetry (ITC), surface plasmon resonance (SPR), or bio-layer interferometry (BLI). Whereas, material shortage, cost, instruments availability, as well as the signal reproduction should be concerned for using these alternative assays. Adding cysteine labeled with fluorescent probe to proteins could be a good option for binding assay and a suitable location of the mutation would be a main problem.

3.3 LAM Localization

To test our hypothesis that LprG may function as a carrier of phosphatidyl inositol-derived glycolipids during their trafficking and delivery to the outer membrane, the LAM localization phenotype of an *M.smegmatis lprG-rv1410c* double knockout strain was elucidated by immunoblotting.

LAM expression was evaluated in *M. smegmatis* wild type mc^2155, Δ*lprG-rv1410c*, and Δ*lprG-rv1410c::MtblprG-rv1410c* strains[13]. No significant difference was detected in whole cell lysate probed with anti-MsmegLAM antibody (Fig. 3-5). This

result suggests that LprG and P55 do not play a critical role in LAM biosynthesis in *M. smegmatis*.

Surprisingly, LAM was found in the outer membrane-enriched fraction for all strains, as detected with either anti-MsmegLAM or anti-Mtb whole cell lysate antibodies (Fig. 3-6). The MsmegLAM blot signal is significantly stronger in the wild-type outer membrane-enriched fraction and qualitatively similar between the knockout and complement strains.

The wild-type strain used as a control, although nominally the same background strain as used for the knockouts, is not from the same stock and may have undergone different selective pressures over repeated passaging in different labs. Such passaging has been shown to result in different genotypes for *M. tb* H37Rv strains[22] and thus may explain the different amounts of LAM detected in the outer membrane-enriched fractions between wild type and complement strains.

Anti-Mtb whole cell lysate can detect LAM, LM, and PIMs. With this antibody, LM was detected in all outer membrane-enriched fractions. For inner membrane-enriched fractions, LM was only detected in wild-type strain. PIM was found in both the inner- and outer-membrane fractions and no significant differences were observed between the three strains. Due to the possible overlap with signals from cross-reacting Antigen 85 proteins, the observed signal may not be attributable only to LAM. Therefore, it may be difficult to observe subtle changes in LAM in the Δ*lprG-rv1410c* knockout strain.

Although a few technical issues need to be solved and experiments need to be repeated, based on these initial data, no significant differences in the location of LAM were observed between the knockout and complement strains. Therefore, it is possible either that LprG and Rv1410c do not function in LAM biosynthesis or transport, or that other proteins may participate in the delivery of LAM to the outer membrane.

Previous studies indicated that knocking out *lprG* or its operon (*lprG-rv1410c*) results in decreased virulence of *M.tb*. Our results imply that this virulence phenotype may not related to membrane integrity or at least may not be directly related to changes in PI-based glycolipids in the membrane.

3.4 Summary and future work

In summary, MtbLprG, V91W MtbLprG, MtbLprA, MsmegLprG, as well as their non-acylated version were cloned and purified from *E. coli*. The differences in binding affinities to lipids were detected by binding with a fluorescent probe (NBD-SA). These proteins were localized to the cell envelope, which is consistent with their prediction as lipoproteins and their hypothesized function in the transport of cell-wall components. However, no significant difference was detected between the *lprG-rv1410c* knockout and complement strains with respect to PIM, LM or LAM localization. As noted above, this suggests that either LprG has some other physiological function or its role in PI-based lipid localization is redundant.

In order to measure the binding affinity of proteins to their putative ligands, other methods will need to be explored. As *M. marinum* is a pathogenic mycobacterial species that is closely related to M. tb and therefore produces lipids that are not made by the more distantly related *M. smegmatis*, other ligands besides those of the PIM family might be detected by expressing our proteins in *M. marinum* and identify the ligands using MS. The localization of LAM will be characterized in additional mutant strains (e.g. single gene knockout strains in *M. smegmatis* and *M. tb*) to test whether LprG and/or P55 influence the biosynthesis and traffic pathway of LAM or other lipids. According to our results, there may be other proteins that participate in this PIM family trafficking pathway. Combined with existing data on LppX, further elucidation of the physiological functions of LprG and LprA will contribute to a general model for lipid transport through the cell wall.

List of Reference

(1) *Global Tuberculosis Report*. World Health Organization: 2012.

(2) Jo, E.-K.; Yang, C.-S.; Choi, C. H.; Harding, C. V. *Cell. Microbiol.* **2007,** *9*, 1087.

(3) Gehring, A. J.; Dobos, K. M.; Belisle, J. T.; Harding, C. V.; Boom, W. H. *J. Immunol.* **2004,** *173*, 2660.

(4) Pecora, N. D.; Gehring, A. J.; Canaday, D. H.; Boom, W. H.; Harding, C. V. *J. Immunol.* **2006,** *177*, 422.

(5) Drage, M. G. Toll-like Receptor 2-Mediated Recognition of Mycobacterial Lipoproteins and Glycolipids. Electronic Thesis or Dissertation, 2009.

(6) Drage, M. G.; Tsai, H.-C.; Pecora, N. D.; Cheng, T.-Y.; Arida, A. R.; Shukla, S.; Rojas, R. E.; Seshadri, C.; Moody, D. B.; Boom, W. H.; Sacchettini, J. C.; Harding, C. V. *Nat Struct Mol Biol* **2010/09,** *17*, 1088.

(7) Jones, B. W.; Means, T. K.; Heldwein, K. A.; Keen, M. A.; Hill, P. J.; Belisle, J. T.; Fenton, M. J. *J. Leukocyte Biol.* **2001,** *69*, 1036.

(8) Nigou, J.; Vasselon, T.; Ray, A.; Constant, P.; Gilleron, M.; Besra, G. S.; Sutcliffe, I.; Tiraby, G.; Puzo, G. *J. Immunol.* **2008,** *180*, 6696.

(9) Pitarque, S.; Larrouy-Maumus, G.; Payré, B.; Jackson, M.; Puzo, G.; Nigou, J. *Tuberculosis* **2008,** *88*, 560.

(10) Dhiman, R. K.; Dinadayala, P.; Ryan, G. J.; Lenaerts, A. J.; Schenkel, A. R.; Crick, D. C. *J. Bacteriol.* **2011,** *193*, 5802.

(11) Sulzenbacher, G.; Canaan, S.; Bordat, Y.; Neyrolles, O.; Stadthagen, G.; Roig-Zamboni, V.; Rauzier, J.; Maurin, D.; Laval, F.; Daffe, M.; Cambillau, C.; Gicquel, B.; Bourne, Y.; Jackson, M. *EMBO J* **2006,** *25*, 1436.

(12) Silva, P. E. A.; Bigi, F.; de la Paz Santangelo, M. a.; Romano, M. I.; Martín, C.; Cataldi, A.; Aínsa, J. A. *Antimicrob. Agents Chemother.* **2001,** *45*, 800.

(13) Farrow, M. F.; Rubin, E. J. *J. Bacteriol.* **2008,** *190*, 1783.

(14) Bigi, F.; Gioffré, A.; Klepp, L.; de la Paz Santangelo, M.; Alito, A.; Caimi, K.; Meikle, V.; Zumárraga, M.; Taboga, O.; Romano, M. I.; Cataldi, A. *Microbes Infect.* **2004,** *6*, 182.

(15) Seeliger, J. C.; Topp, S.; Sogi, K. M.; Previti, M. L.; Gallivan, J. P.; Bertozzi, C. R. *PLoS ONE* **2012,** *7*, e29266.

(16) Stover, C. K.; de la Cruz, V. F.; Fuerst, T. R.; Burlein, J. E.; Benson, L. A.; Bennett, L. T.; Bansal, G. P.; Young, J. F.; Lee, M. H.; Hatfull, G. F.; Snapper, S. B.; Barletta, R. G.; Jacobs, W. R.; Bloom, B. R. *Nature* **1991,** *351*, 456.

(17) Rezwan, M.; Lanéelle, M.-A.; Sander, P.; Daffé, M. *J. Microbiol. Methods* **2007,** *68*, 32.

(18) Niederweis, M.; Ehrt, S.; Heinz, C.; Klöcker, U.; Karosi, S.; Swiderek, K. M.; Riley, L. W.; Benz, R. *Mol. Microbiol.* **1999,** *33*, 933.

(19) Seeliger, J. C.; Holsclaw, C. M.; Schelle, M. W.; Botyanszki, Z.; Gilmore, S. A.; Tully, S. E.; Niederweis, M.; Cravatt, B. F.; Leary, J. A.; Bertozzi, C. R. *J. Biol. Chem.* **2012,** *287*, 7990.

(20) Prados-Rosales, R.; Baena, A.; Martinez, L. R.; Luque-Garcia, J.; Kalscheuer, R.; Veeraraghavan, U.; Camara, C.; Nosanchuk, J. D.; Besra, G. S.; Chen, B.; Jimenez, J.;

Glatman-Freedman, A.; Jacobs, W. R.; Porcelli, S. A.; Casadevall, A. *J. Clin. Invest.* **2011,** *121*, 1471.

(21) Roehrl, M. H. A.; Wang, J. Y.; Wagner, G. *Biochemistry* **2004,** *43*, 16056.

(22) Ioerger, T. R.; Feng, Y.; Ganesula, K.; Chen, X.; Dobos, K. M.; Fortune, S.; Jacobs, W. R.; Mizrahi, V.; Parish, T.; Rubin, E.; Sassetti, C.; Sacchettini, J. C. *J. Bacteriol.* **2010,** *192*, 3645.

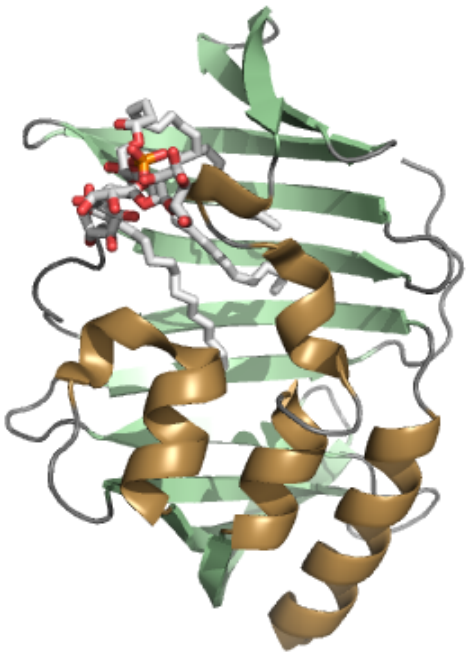

Figure 1-1. Crystal structure of NA-MtbLprG with Ac_1PIM_2. (PDB ID: 3MHA)

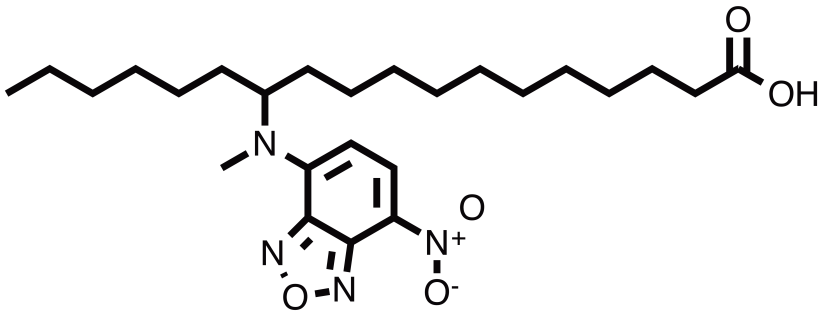

Figure 2-1. 12-N-methyl-(7-nitrobenz-2-oxa-1,3-diazo) aminostearic acid (NBD-SA)

a. Full-length lipoproteins

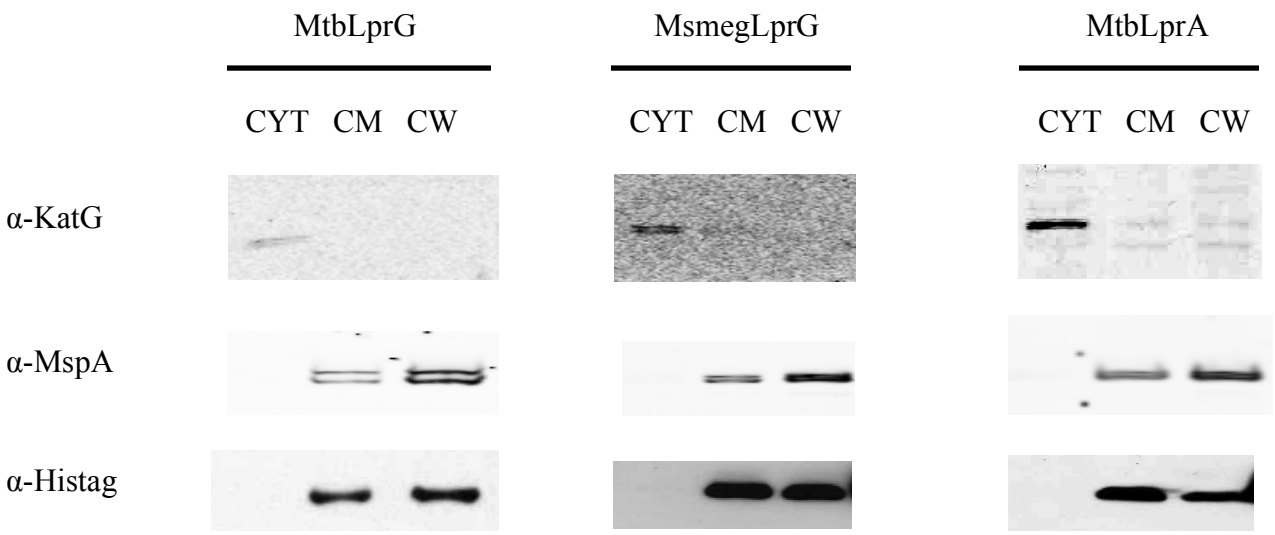

b. Non-acylated lipoproteins

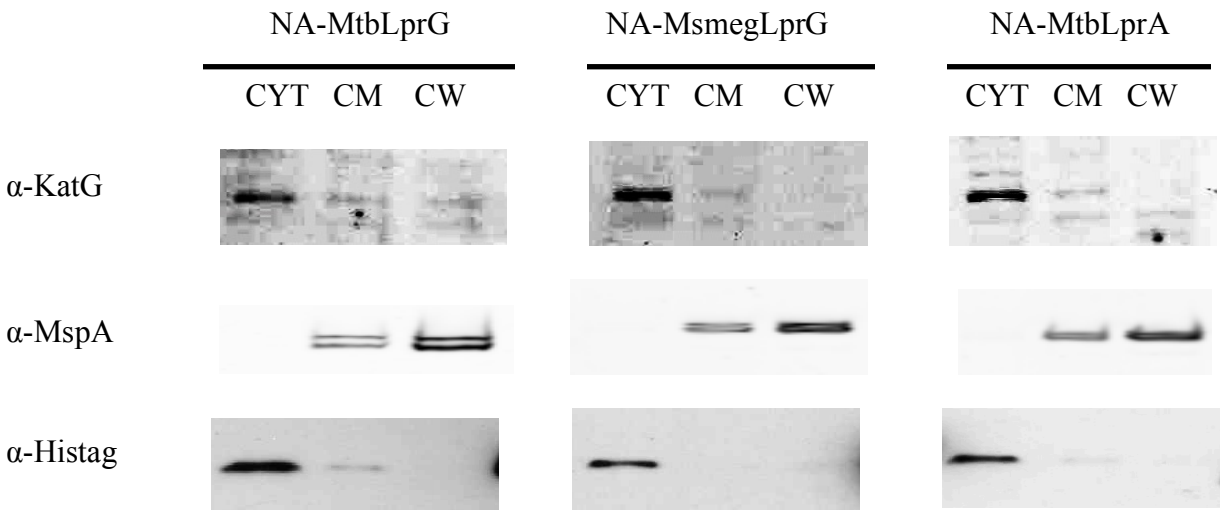

Figure 3-1. Full-length lipoproteins were all detected in the cytosolic membrane- and cell wall-enriched fractions using the differential centrifugation fractionation method (a). Non-acylated lipoproteins were detected in cytosol-enriched fraction using the differential centrifugation fractionation method (b).

Table 3-1. The dissociation constants (K_d) of NBD-SA to the non-acylated lipoproteins

Protein	NA-MtbLprG	V91W NA-MtbLprG	NA-MsmegLprG	NA-MtbLprA
Kd (μM)	5±1.1	6±1.6*	26±10.8/72±29.4*	10±3.2/2.3±0.7*

* Using 2-fold dilution method

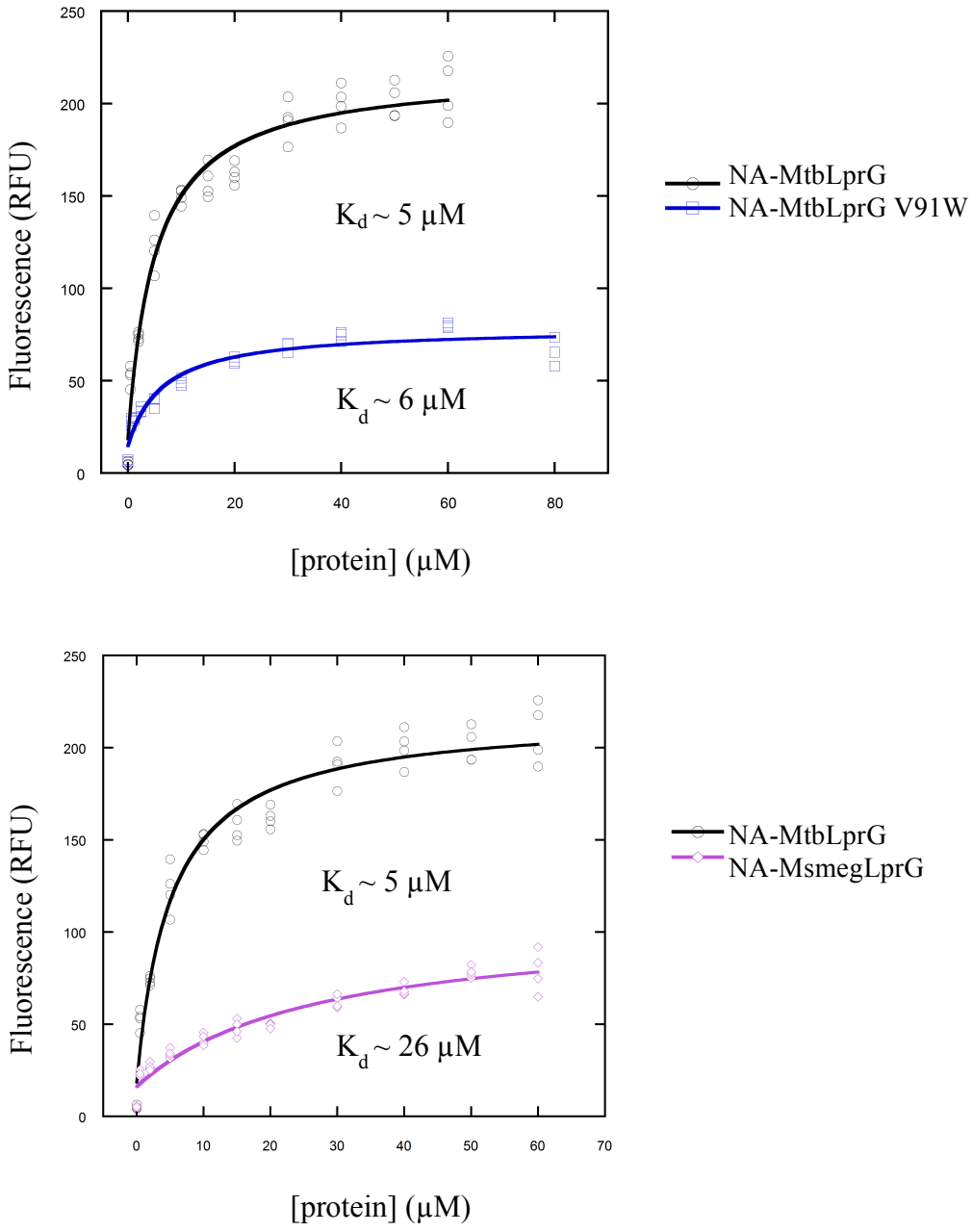

Figure 3-2. NA-MtbLprG (K_d=5±1.1 μM) and V91W mutated NA-MtbLprG (K_d=6±1.6 μM) bind to NBD-SA with comparable dissociation constants. The fluorescent probe binds more tightly to NA-MtbLprG (K_d=5±1.1 μM) than to MsmegLprG (K_d=26±10.8 μM). The binding curves were fit the equation: $y=m_3+m_2\times m_0/(m_1+m_0)$ (y, fractional occupancy; m_0, protein concentration; m_1, K_d; m_2, scale factor) using Kaleidagraph (Synergy Software)

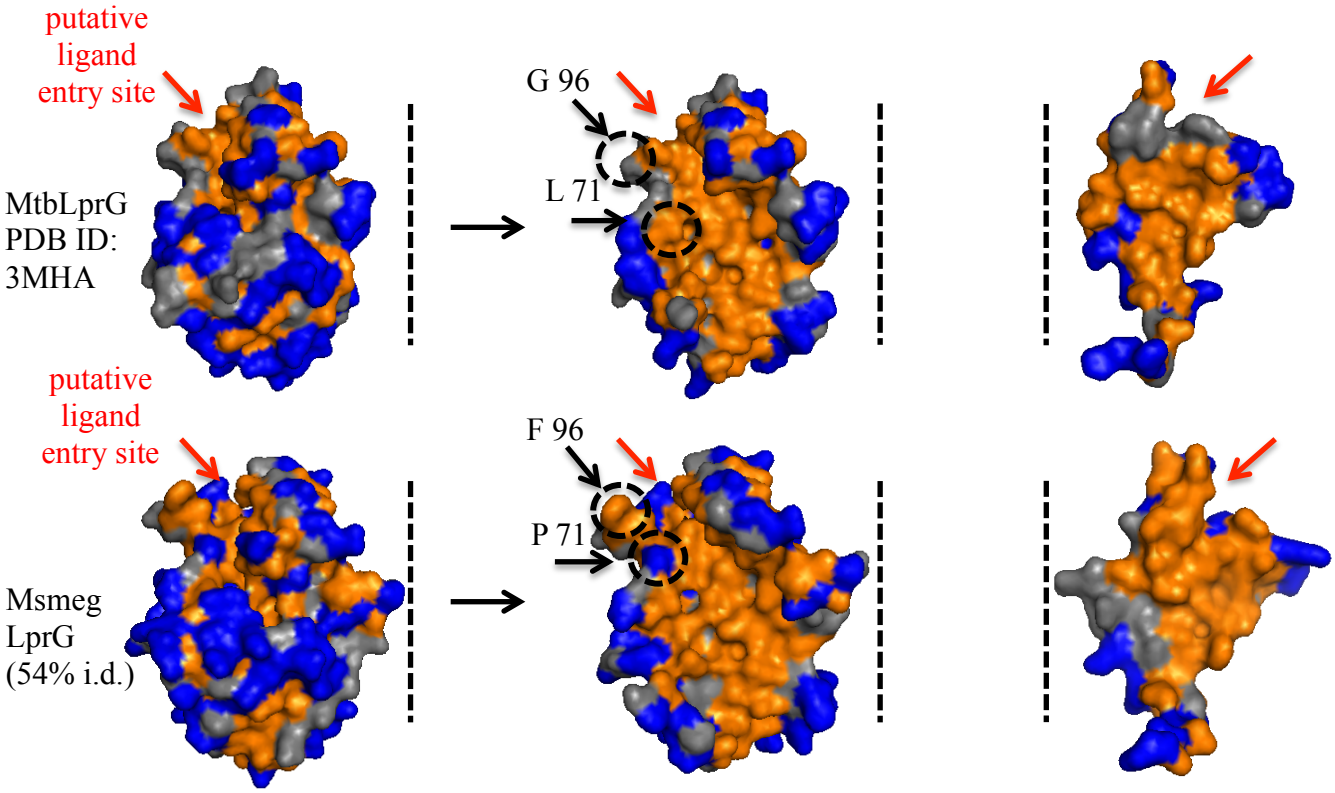

Figure 3-3. The surface inside the expected binding pocket of MtbLprG (PDB ID: 3MHA) and MsmegLprG (structure prediction generated using the Phyre2 server using MtbLprG as template). (Grey: neutral residues; Yellow: hydrophobic residues; Blue: hydrophilic residues)

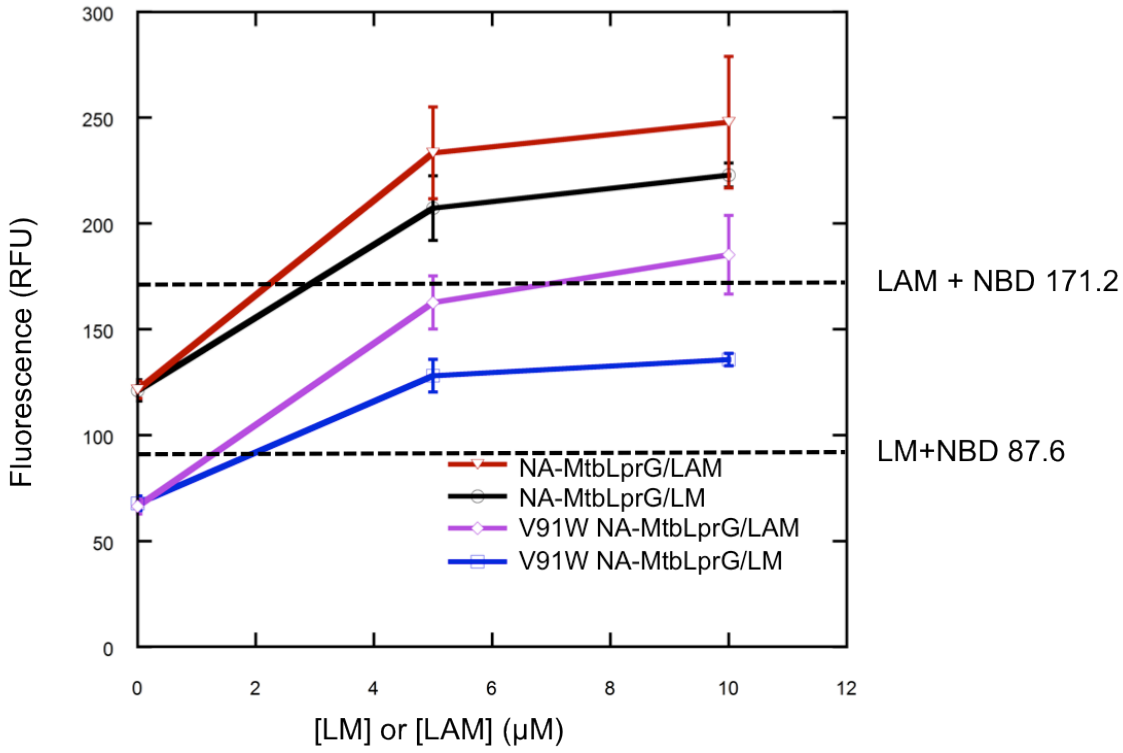

Figure 3-4. Competitive binding of NA-MtbLprG with MtbLM, MtbLAM, as well as the binding of V91W NA-MtbLprG with MtbLM and MtbLAM, were measured.

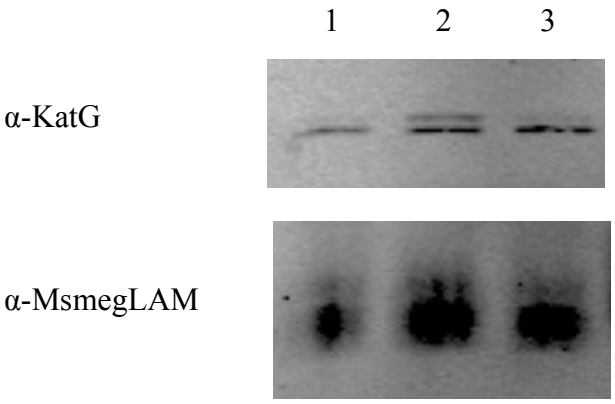

Figure 3-5. No significant difference in LAM expression level was detected using whole cell lysate probed with anti-MsmegLAM antibody. 1) *M. smeg* wild type mc^2155, 2) *M. smeg ΔlprG-rv1410c,* 3) *M. smeg ΔlprG-rv1410c::MtblprG-rv1410c*

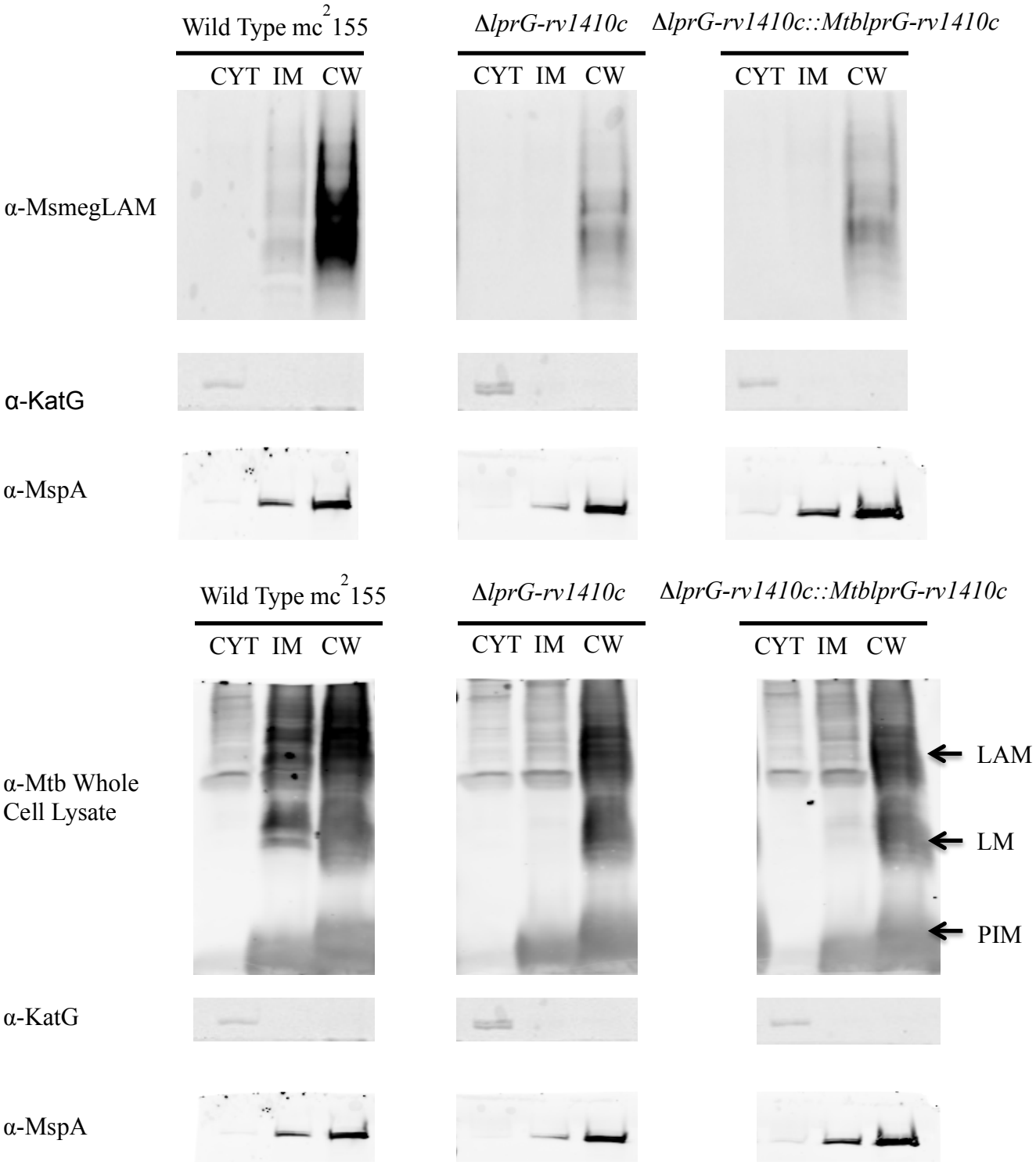

Figure 3-6. LAM was found in the outer membrane-enriched fraction for all strains, as detected with either anti-MsmegLAM or anti-Mtb whole cell lysate antibodies.

Appendix

Table 1. Primer Sequences and Cloning Methods

Name	Primer Sequence	Method
2BT_Hisx6-TEV-MtbLprG_(MSMEG_3070)	5' primer TACTTCCAATCCAATCAGACGCGCCCACGCTTCG	InFusion SspI
	3' primer TATCCACTTCCAATTCAGGCCGCGGGCTTGG	
pET24b_MtbLprG-TEV-6xHis_(Mtb_Rv1141c)	5' primer AAGAAGGAGATATACATATGCGGACCCCCAGACG	InFusion NdeI HindIII
	3' primer GTGCGGCCGCAAGCTTGGATTGGAAGTACAGGTTTTCGCTCACCGGGGGCTTC	
pET24b_V91W_MtbLprG-TEV-6xHis_(Mtb_Rv1141c)	5' primer GCCGCGACGGGAAACTGGAAGCTCACGCTGGGT	Site-directed mutagenesis
	3' primer ACCCAGCGTGAGCTTCCAGTTTCCCGTCGCGGC	
pET24b_LprA-TEV-6xHis_(Mtb_Rv1270c)	5' primer AAGAAGGAGATATACATATGAAGCATCCACCTTGTTCCG	InFusion NdeI HindIII
	3' primer GTGCGGCCGCAAGCTTGGATTGGAAGTACAGGTTTTCGACCGGTTTGGTGGCGG	
pET24b_MsmegLprG-TEV-6xHis_(MSMEG_3070)	5' primer AAGAAGGAGATATACATATGCAGACGCGCCCACGC	InFusion NdeI HindIII
	3' primer GTGCGGCCGCAAGCTTGGATTGGAAGTACAGGTTTTCGGCCGCGGGCTTGG	
pET24b_NA-MtbLprG-TEV-6xHis_(Mtb_Rv1141c)	5' primer AAGAAGGAGATATACATATGTCGTCGGGCTCGAAGCC	InFusion NdeI HindIII
	3' primer GTGCGGCCGCAAGCTTGGATTGGAAGTACAGGTTTTCGCTCACCGGGGGCTTC	
pET24b_V91W_NA-MtbLprG-TEV-6xHis_(Mtb_Rv1141c)	5' primer GCCGCGACGGGAAACTGGAAGCTCACGCTGGGT	Site-directed mutagenesis
	3' primer ACCCAGCGTGAGCTTCCAGTTTCCCGTCGCGGC	
pET24b_NA-MtbLprA-TEV-6xHis_(Mtb_Rv1270c)	5' primer AAGAAGGAGATATACATATGTCAACCGAAGGGGACGCC	InFusion NdeI HindIII
	3' primer GTGCGGCCGCAAGCTTGGATTGGAAGTACAGGTTTTCGACCGGTTTGGTGGCGG	
pET24b_NA-MsmegLprG-TEV-6xHis_(MSMEG_3070)	5' primer AAGAAGGAGATATACATATGTCGTCGTCATCGGAGACCTCC	InFusion NdeI HindIII
	3' primer GTGCGGCCGCAAGCTTGGATTGGAAGTACAGGTTTTCGGCCGCGGGCTTGG	
pRibo EcoHind_MtbLprG-TEV-6xHis_(Mtb_Rv1141c)	5' primer AAGGAGGCAACAAGATGGCCAGCCGGACCCCCAGACGCC	InFusion MscI EcoRI
	3' primer GACATCGATAAGCTTGAATTCCTTTGTTAGCAGCCGGATCTCAGTG	
pRibo EcoHind_MtbLprA-TEV-6xHis_(Mtb_Rv1270c)	5' primer AAGGAGGCAACAAGATGGCCAGCAAGCATCCACCTTGTTCCGTTG	InFusion MscI EcoRI
	3' primer GACATCGATAAGCTTGAATTCCTTTGTTAGCAGCCGGATCTCAGTG	
pRibo EcoHind_MsmegLprG-TEV-6xHis_(MSMEG_3070)	5' primer AAGGAGGCAACAAGATGGCCAGCCAGACGCGCCCACGC	InFusion MscI EcoRI
	3' primer GACATCGATAAGCTTGAATTCCTTTGTTAGCAGCCGGATCTCAGTG	
pRibo EcoHind_NA-MtbLprG-TEV-6xHis_(Mtb_Rv1141c)	5' primer AAGGAGGCAACAAGATGGCCAGCTCGTCGGGCTCGAAGCC	InFusion MscI EcoRI
	3' primer GACATCGATAAGCTTGAATTCCTTTGTTAGCAGCCGGATCTCAGTG	
pRibo EcoHind_NA-MtbLprA-TEV-6xHis_(Mtb_Rv1270c)	5' primer AAGGAGGCAACAAGATGGCCAGCTCAACCGAAGGGGACGCC	InFusion MscI EcoRI
	3' primer GACATCGATAAGCTTGAATTCCTTTGTTAGCAGCCGGATCTCAGTG	
pRibo EcoHind_NA-MsmegLprG-TEV-6xHis_(MSMEG_3070)	5' primer AAGGAGGCAACAAGATGGCCAGCTCGTCGTCATCGGAGACCTCC	InFusion MscI EcoRI
	3' primer GACATCGATAAGCTTGAATTCCTTTGTTAGCAGCCGGATCTCAGTG	
pMV261_MtbLprG-TEV-6xHis_(Mtb_Rv1141c)	5' primer GGAATCACTTCGCAATGGCCAGCCGGACCCCCAGACGCC	InFusion MscI EcoRI
	3' primer ACATCGATAAGCTTCGAATTCCTTTGTTAGCAGCCGGATCTCAGTG	
pMV261_V91W MtbLprG-TEV-6xHis_(Mtb_Rv1141c)	5' primer GGAATCACTTCGCAATGGCCAGCCGGACCCCCAGACGCC	InFusion MscI EcoRI
	3' primer ACATCGATAAGCTTCGAATTCCTTTGTTAGCAGCCGGATCTCAGTG	
pMV261_MsmegLprG-TEV-	5' primer GGAATCACTTCGCAATGGCCAGCCAGACGCGCCCACGC	InFusion MscI

6xHis_(MSMEG_3070)	3' primer ACATCGATAAGCTTCGAATTCCTTTGTTAGCAGCCGGATCTCAGTG	EcoRI
pMV261_NA-MtbLprG-TEV-6xHis_(Mtb_Rv1141c)	5' primer GGAATCACTTCGCAATGGCCAGCTCGTCGGGCTCGAAGCC	InFusion MscI
	3' primer ACATCGATAAGCTTCGAATTCCTTTGTTAGCAGCCGGATCTCAGTG	EcoRI
pMV261_V91W NA-MtbLprG-TEV-6xHis_(Mtb_Rv1141c)	5' primer GGAATCACTTCGCAATGGCCAGCTCGTCGGGCTCGAAGCC	InFusion MscI
	3' primer ACATCGATAAGCTTCGAATTCCTTTGTTAGCAGCCGGATCTCAGTG	EcoRI
pMV261_NA-MsmegLprG-TEV-6xHis_(MSMEG_3070)	5' primer GGAATCACTTCGCAATGGCCAGCTCGTCGTCATCGGAGACCTCC	InFusion MscI
	3' primer ACATCGATAAGCTTCGAATTCCTTTGTTAGCAGCCGGATCTCAGTG	EcoRI

Table 2. Protein Expression and Purification

Name	Theoretical Extinction Coefficient (M^{-1} cm^{-1})	Protein Expression				Protein Purification			MS Verification
		Temperature	[IPTG]	Time	Scale	Nickel Affinity	Anion Exchange	Size Exclusion	
MtbLprG	21095	18°C	0.1mM	16h	2mL/50mL/ 1L	✔	pH=8.4 (Theoretical pI=7.13)	✔	✖
V91W MtbLprG	26595	18°C	0.1mM	16h	2mL	–	–	–	–
MtbLprA	18575	37°C	0.1mM	4h	2mL/50mL/ 1L	✔	✖	✔	✔
MsmegLprG	17023	18°C	0.1mM	16h	2mL/50mL/ 1L	✔	pH=7.4 (Theoretical pI=4.93)	✔	✖
NA-MtbLprG	20970	37°C	0.1mM	4h	2mL/1L	✔	✖	✔	✔
V91W NA-MtbLprG	26470	37°C	0.1mM	4h	2mL/1L	✔	✖	✔	✔
NA-MtbLprA	18450	37°C	0.1mM	4h	2mL/1L	✔	✖	✔	✔
NA-MsmegLprG	16500	37°C	0.1mM	4h	2mL/1L	✔	✖	✔	✔